ELSEVIER

Polymer 41 (2000) 6223–6230

polymer

Preparation of high performance poly(ethylene terephthalate) fibers: two-stage drawing using high pressure CO_2

T. Hobbs, A.J. Lesser*

Department of Polymer Science and Engineering, Box 34530, University of Massachusetts, Amherst, MA 01003, USA

Received 4 August 1999; received in revised form 17 November 1999; accepted 18 November 1999

Abstract

Poly(ethylene terephthalate) fibers were drawn in CO_2 (liquid) at 23°C above the critical pressure followed by a second stage draw $\geq$ 200°C in air. We investigated the effects of first stage morphology on the second stage drawability and properties of the resultant fibers after the second stage. At 200°C, the maximum achievable draw ratios (DR_{max}) for the CO_2 treated and untreated original fibers were 12.2 and 8.2, respectively. The CO_2 treated fibers had 10% higher strength and modulus values. In addition, the CO_2 treated fibers showed slightly higher birefringence and crystallinity values. At higher draw temperatures, the fibers had high crystallinity values (>60%). However, the amorphous chain orientation was much lower. The high drawability of the PET drawn in CO_2 can be explained by the plasticization of the polymer where CO_2 aids in the disentanglement of the polymer chains during the drawing process. This CO_2 morphology results in a very ductile structure compared to untreated fibers.

Keywords: Carbon dioxide; Poly (ethylene terephthalate); Fibers

1. Introduction

The production of high modulus and high strength fibers has been the subject of intense research over the past few years. Poly(ethylene terephthalate) (PET) is one of the most important fibers for industrial production. Because of its high performance, low cost, and recycleability, it is one of the most attractive candidates for high strength fibers. A large number of experimental techniques have been investigated for improving PET including solid state coextrusion, zone drawing, microwave heating, and vibrational hot drawing [1–4]. The most successful techniques for drawing ultrahigh molecular weight PET fibers use solution spinning techniques where the entanglement density is low [5,6]. These processes are undesirable because of the use of organic solvents of which many are toxic and expensive.

Conventional melt spun PET fibers have limited mechanical properties attributed to the relatively low molecular weight of the polymer. Ultra high molecular weight PET cannot be melt spun because of the extremely high viscosity of the melt. As an alternative, high performance fibers can be made using a post-treatment process. It has been shown that organic solvents such as DMF or acetone induce a morphology that enhances the drawability which results in higher strength and modulus fibers [7,8]. For example, fibers treated with acetone could be drawn to higher draw ratios (11.5 vs. 9.5). These fibers had strength and modulus values that were 20% higher compared to untreated fibers. The morphology of these fibers is extremely complex. Acetone initially plasticizes and crystallizes the amorphous fiber creating small and/or imperfect crystallites.

We have shown previously that CO_2 can be used to enhance the drawability of PET fibers in a single stage drawing process [9]. Fibers could be drawn in CO_2 to higher draw ratios with a comparable increase to fibers treated with DMF/H_2O. During the drawing process, CO_2 significantly enhanced the development of the crystalline phase. Pressure dramatically affected the drawing behavior and the maximum achievable draw ratio during the first stage. Higher pressures caused premature fiber failure attributed to crystallization, which limited deformation.

Initially amorphous fibers drawn in a one-stage drawing process in subcritical or liquid CO_2 showed a distinct morphology. These fibers had much lower birefringence values compared to cold drawn fibers, 0.15 and 0.19, respectively [9]. Hence, the total orientation of the fibers was significantly lower due to the plasticizing effect of the CO_2. In situ mechanical measurements showed that the polymer was above its glass transition temperature. In addition, we believe that the entanglement density of the CO_2 drawn fibers was lower due to the enhanced mobility of the

* Corresponding author. Tel.: +1-413-577-1316; fax: +1-413-545-0082.
E-mail address: ajl@polysci.umass.edu (A.J. Lesser).

0032-3861/00/$ - see front matter
PII: S0032-3861(99)00849-6

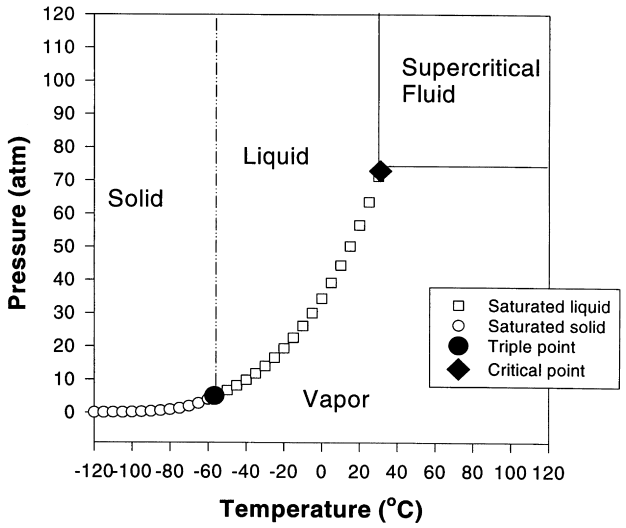

Fig. 1. Phase diagram for CO_2.

polymer chains allowing for disentanglement. The CO_2 drawn fibers had 10% higher crystallinity values compared to the cold drawn fibers. However, the volume percent crystallinity values were still low being less than 30%.

Compared to other processing methods, tensile drawing in CO_2 is unique because CO_2 is both a plasticizer and a pressure transmitting media. Upon depressurization, CO_2 escapes from the polymer substrate. Hence, it acts as a *reversible plasticizer*. The concept of reversible plasticization was originally developed by Zachariades and Porter using NH_3 during the solid state extrusion of nylon 6 and nylon 6,6 [10].

Compared to traditional or uniaxial drawing, drawing in CO_2 can place the polymer fiber in a multi-axial stress state under certain process conditions, i.e. no permeation of the polymer. Under nonpermeable conditions, our process mimics solid state extrusion or drawing in pressurized silicone oil. Under conditions of good permeability and sorption, the process is similar to Ito's solvent treatment. These conditions and transport properties of CO_2 can readily be tuned by changing pressure and/or temperature. It is widely accepted that CO_2 cannot permeate the crystalline component of polymers, hence the crystalline component is under hydrostatic stress. Upon drawing, permeability of the CO_2 in the amorphous phase can change as the chains orient into a more densely packed state. This is a known phenomenon for other polymer systems [11]. Overall, drawing in CO_2 is a unique process pressurizing the crystalline phase.

Ito et al. has shown that a two-stage drawing process is favorable for preparing high strength PET fibers [5]. They showed that the initial morphology created in the first stage draw is extremely important with regard to properties achieved after the second stage draw [12]. In this paper, we will investigate the drawing behavior of PET in a concentrated region (44–102 atm) near the critical pressure at 23°C. This is below the critical temperature. This region is show on a phase diagram in Fig. 1. The main purpose of this paper is to investigate fibers and their resultant structure after drawing at a high temperature. Hence, we will investigate a two-stage drawing technique where the first stage is performed in high pressure CO_2 (CO_2 treated) or air for comparison, and the second stage is performed ≥ 200°C in air. We will discuss the morphology and structural development in the amorphous and crystalline phases along with tensile properties.

2. Experimental

2.1. Samples

Initially amorphous, unoriented PET fibers were prepared using a Randcastle microextruder with a die temperature of 295°C. The intrinsic viscosity (50/50 trichloracetic acid/dichloromethane at 30°C) of the fiber grade polymer chip prior to spinning was 1.18 dl/g. The fibers were shown to be amorphous by Differential Scanning Calorimetry (DSC) and WAXD and had an initial birefringence of 1.5×10^{-3}. A two-stage draw technique was used for both treated and untreated original fibers. For the treated fibers, the amorphous fibers were drawn in CO_2 after a soak period of 15 min at a given pressure and a strain rate of $1\ min^{-1}$ using a custom high pressure apparatus. For untreated fibers, the fiber bundles were drawn in air at ambient conditions at the same strain rate. The second stage draw for both untreated and treated fibers was conducted ≥ 200°C in a convection air oven.

2.2. Draw techniques

The first stage draw of the CO_2 treated fibers was performed in a custom high pressure drawing apparatus. The apparatus is mounted on an Instron model 1333 tensile testing machine. Coleman grade CO_2 is supplied through a Hydro-pac, Inc. high-pressure carbon dioxide pump and filtered through activated carbon and a drying agent. The apparatus is capable of making in situ force measurements using a calibrated stainless steel cantilever beam and a linear variable displacement transducer (LVDT) with electronics outside of the CO_2 media. The electronic signals and crosss-head displacement are monitored using a personal computer using MTS Teststar II software. Stress values were calculated from force measurements normalized by the fiber cross sectional area. The initial cross sectional area was determined from the linear density of the bundles and the amorphous fiber density of $1.325\ g/cm^3$. Strain was calculated from the relative displacement between the crosshead and beam normalized by the fiber gage length. Draw ratios were directly calculated from the strain measurements. All fiber bundles unless otherwise specified were drawn at a strain rate of $1\ min^{-1}$.

The second stage draw was conducted in a high temperature convection air oven chamber on an Instron 1233. The

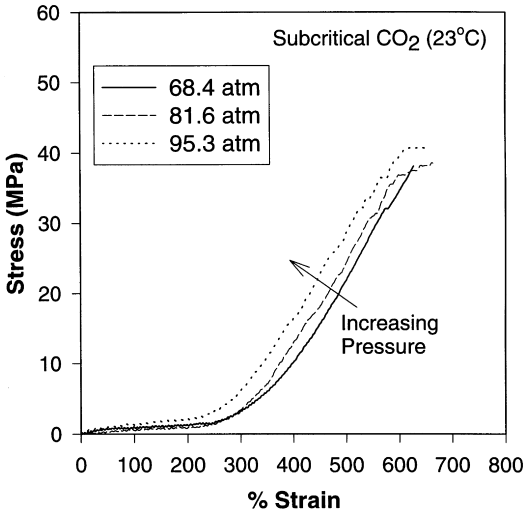

Fig. 2. Drawing of PET fibers in liquid CO_2.

second stage draw unless otherwise specified was conducted at 200°C. For higher temperatures, the fibers were dried for 30 h at 50°C to prevent hydrolysis. Fibers were drawn under constant strain rate until individual filaments began failing as the load reached a plateau. The crosshead was stopped and the fibers were held under a high load during cooling in order to preserve or maximize amorphous orientation. During cooling, the load would decrease when the crosshead was stopped and then increase upon further cooling near 130°C.

2.3. Measurements

Single filament tests were performed on an Instron 5564 or 1123 at a strain rate of 0.1 min^{-1} and a gauge length of 25 mm. Specimens were tabbed onto a cardboard template using an epoxy adhesive. The fiber diameter was measured using a high magnification microscope calibrated with a micrometer scale. Birefringence measurements were made using an Olympus polarizing microscope equipped with a 1–20λ Berek compensator. Crystallinity measurements were made using a density column prepared from *n*-heptane and CCl_4. Volume percent crystallinity was calculated based on a two-phase model using densities of 1.333 and 1.455 g/cm^3 for the amorphous and crystalline phases, respectively [13]. DSC was performed using a TA Instruments thermal analyst 2100 with a heating rate of 10°C/min. Flat plate X-ray diffraction patterns were obtained using a Rigura Statton camera (40 kV, 30 mA) under vacuum conditions. Evaluation of the crystal orientation function was made by scanning the negatives using a rotating colorimeter to obtain azimuthal angle vs. intensity plots for the $(\bar{1}05)$ plane. The f_c was measured by a well-known X-ray diffraction method [14]. The amorphous orientation, f_a was calculated by combining the optical birefringence data with f_c and sample crystallinity [14]. The intrinsic birefringences of the crystal and amorphous phases were taken to be 0.220 and 0.275, respectively [15].

3. Results and discussion

3.1. One-stage drawing

Previously, we investigated the drawing behavior of amorphous PET over a wide range of CO_2 pressures at 68 atm intervals [9]. Maximum drawability occurred near the critical pressure. We have performed further drawing experiments at small pressure intervals (13.6 atm) below and above the critical pressure. The experimental details and apparatus have been reported previously [9]. Fig. 2 shows the stress/strain plots at various pressures near the critical pressure which is 72.8 atm. The in situ drawing behavior is very similar throughout the pressure range. However, the stress/strain curve shifts to the left as the CO_2 pressure is increased. The fibers are completely plasticized and show no yield point. At 300% strain, the fibers show a region of strain hardening attributed to crystallization and further orientation. The maximum achievable draw ratio for these fibers is 7.6, i.e. 660% strain where individual filaments begin failing. It is interesting to note that the fibers are still drawable even at 102.1 atm (curve not shown), well above the critical pressure.

Passing above the critical temperature does not affect the drawing behavior. Fibers drawn in supercritical conditions (88.5 atm, 35°C) show similar drawing behavior to fibers drawn below the critical temperature at the same pressure. The drawing behavior is very similar to the stress vs. strain curves shown in Fig. 2. Although the CO_2 enters the supercritical state, it does not significantly affect the drawing behavior. This is somewhat surprising as the density and transport properties of CO_2 change significantly when passing from a liquid to a supercritical state.

The structure of the fibers drawn above the critical pressure is similar to what we reported previously for fibers drawn below the critical pressure [9]. Compared to cold drawn fibers, fibers drawn in the liquid CO_2 (subcritical) had significantly lower birefringence values. The lower birefringence and overall chain orientation can be attributed to relaxation and segmental motion of the polymer chains in the presence of CO_2. Hence, after the first stage of drawing, fibers in CO_2 have an overall lower degree of orientation despite the fact that they were drawn to higher ratio. Overall, this suggests that drawing process in CO_2 may be less efficient but results in fibers with a unique morphology.

It has been shown that the morphology of PET fibers prior to a second stage draw is one of the most important factors for preparing high strength fibers. For acetone treated samples, a total draw ratio of 11.5 vs. 9.5 could be achieved because of the acetone plasiticizing and inducing the formation of small and/or imperfect crystallites [16].

The morphology for CO_2 treated fibers is believed to be

Table 1
Comparison of draw ratios achieved by various techniques

Treatment	Temperature (°C)	DR_1	DR_2	TDR
Untreated	200	6.0	1.36	8.2
CO_2 treated	200	7.6	1.60	12.2
CO_2 treated	230	7.6	1.90	14.4
Acetone	230	7.0	1.64	11.5
DMF/H_2O	230	7.0	1.64	11.5

less complex because of the extremely fast diffusion of the CO_2 and slow crystallization. The crystallization of PET occurs in two distinct limiting modes [17]. In the first, the solvent penetrates the polymer inducing crystallization creating a barrier, which slows further diffusion of the solvent. An advancing front can be detected separating the amorphous unpenetrated core and crystallized outer layers. The crystallization process is kinetically faster than the diffusion and sorption process. This process occurs for PET upon treatment with traditional solvents such as acetone and aromatic hydrocarbons.

In the second mode, PET is completely saturated by the solvent followed by crystallization where the kinetic rate of crystallization is usually slow. The second mode describes the crystallization of PET with CO_2 gas. We believe that the same mode occurs at higher pressures as well. This contention for complete plasticization is supported by high diffusion constants for CO_2 at elevated pressures and the observed gross macroscopic shrinkage of fiber bundles observed after CO_2 treatment (40–204 atm) [9]. If the fiber bundles crystallized prior to complete penetration, macroscopic shrinkage would not be observed. The initial morphology of the acetone treated fibers is extremely complex because of the slow diffusion and fast crystallization processes. The outer shell of the fiber crystallizes under different conditions compared to the core of the fiber. In contrast, one would expect the CO_2 treated fibers to be nearly homogenous in the radial direction as a result of high diffusion rates and slow crystallization. The resultant morphology is inherently less complex.

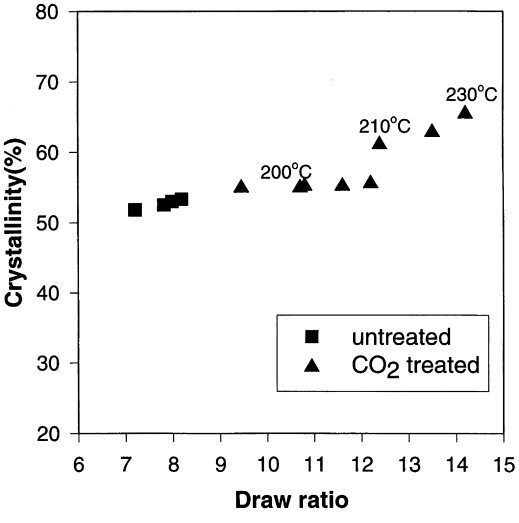

Fig. 3. Volume percent crystallinity dependence on draw ratio.

3.2. Drawability

The total draw ratio (TDR) achieved by a two-stage drawing technique was calculated by the following equation:

$$TDR = DR_1 \times DR_2 \quad (1)$$

DR_1 is the draw ratio achieved in the first stage and DR_2 is the draw ratio achieved in the second stage. The draw ratios in each stage were calculated directly from strain measurements. Generally, draw ratios calculated from strain measurements are greater when compared to draw ratios measured from the separation of lateral ink marks. This is due to the necking that occurs in the first stage. Achieving a higher draw ratio in either the first stage or second stage can increase the TDR according to Eq. (1). The increase in drawability for solvent treated fibers generally occurred during the first stage [18]. For CO_2 treated fibers, the drawability increased in both stages compared to untreated fibers. We previously reported 30% increase in drawability using CO_2, a similar increase to DMF/water treatments in the first stage. We have observed that an increase in drawability occurs in the second stage drawing process as well. These results for CO_2 treated fibers are compared to cold drawn (untreated) and solvent treated fibers in Table 1. The DR_2 for CO_2 fibers at 200°C was 1.6 compared to 1.36 for untreated fibers. The TDR achieved for CO_2 drawn fibers, 12.2 compared to untreated fibers, 8.2 is approximately 50% higher. At higher temperatures, higher TDR values are obtained for CO_2 treated fibers compared to treatments with traditional organic solvents. We believe that the enhanced drawability can be related to the lower entanglement density after one-stage drawing. Overall, CO_2 appears to be the most effective method for attaining maximum draw ratios.

3.3. Microstructure of two-stage drawn fibers

The two-stage drawn PET fibers were physically characterized by various methods to further investigate their structure at smaller length scales. WAXD, birefringence, and crystallinity measurements were used to calculate orientation functions for the amorphous and crystalline phases, f_a and f_c, respectively. In general, the CO_2 treated PET fibers have slightly higher crystallinity values compared to untreated fibers and achieved the same level of orientation.

The volume percent crystallinity (X_v) as a function of draw ratio for both the untreated and treated fibers is shown in Fig. 3. The crystallinity increases slightly with TDR. At a treatment temperature of 200°C, the CO_2 treated fibers have a crystallinity of 55.5% compared to 53.1% for the untreated fibers. The crystallinity of the treated fibers at higher draw ratios is increased substantially to 65.4% at a drawing temperature of 230°C. To attain 65% crystallinity,

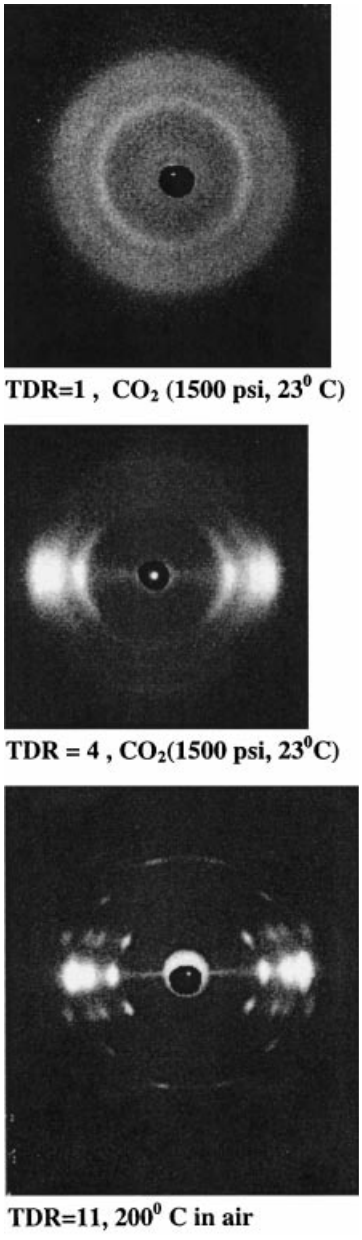

Fig. 4. Evolution of the crystalline phase during the drawing process.

untreated fibers have to be annealed under tension for 2–3 h. This annealing process is accompanied by an undesirable decrease in molecular weight resulting in poor tensile strength [19].

The use of CO_2 in the first drawing stage aids in the development of the crystalline phase. This is exemplified by the WAXD flat plate patterns in Fig. 4. Even before the fibers are drawn (DR = 1), a 15 min treatment above the critical pressure at 23°C results in the formation of diffuse rings in the diffraction pattern indicating the formation of small/imperfect crystallites. We believe that a significant amount of the crystallization occurs upon depressurization or CO_2 removal from the polymer. For the drawing studies, the fibers used were initially amorphous. CO_2 treatment alone at 23°C induces crystallization as indicated by WAXD. The as-spun fibers do crystallize much faster compared to isotropic films because of network stretch and residual stress that exists in the fibers from the spinning process. The as-spun fibers have very low orientation, but do shrink significantly when heated above their T_g. DSC analysis indicates that isotropic films do not crystallize under the pressure range studied in the 15 min time period. CO_2 treated fibers do crystallize as evident by disappearance of the crystallization exotherm and WAXD patterns as discussed previously. After the fibers are drawn to the strain hardening point (DR $\sim$ 4), the WAXD patterns show significant orientation as one would expect. The rings in the diffraction pattern are still diffuse indicating an imperfect crystal structure. Further drawing and heat treatment result in a well-defined pattern characteristic of oriented PET fibers. The crystalline reflections become significantly sharper as the crystalline regions increase in size and perfection. The resultant fibers are highly oriented with a crystalline orientation function, $f_c > 0.9$.

Fig. 5 shows the change in the measured birefringence for fibers drawn under constant strain rate at 200°C. Birefringence represents an overall orientation of the polymer chains. The maximum birefringence (0.228) obtained for the treated fibers is just slightly higher compared to untreated fibers (0.226) indicating only a slightly higher orientation. It should be noted that these fibers were drawn in the first stage above the critical pressure for CO_2. The arrow in Fig. 5 shows the combined effect of the heat treatment and further drawing in the second stage. The birefringence increases substantially and the crystallinity values nearly double. The birefringence of the first stage drawn fibers is quite low being <0.15. The development of orientation occurs much more rapidly for untreated fibers over a small draw ratio range. For CO_2 treated fibers, the birefringence increases more slowly and attains only a slightly higher mean value.

Fig. 6 shows the TDR dependence on the chain orientation factors for the crystalline and amorphous regions for the two-stage drawn fibers at 200°C. The f_c values of the samples are very similar and stay an almost constant value of 0.915. This behavior has been reported previously for different two-stage drawn PET systems [5,20]. It is a general behavior for many polymer systems. The f_a values increase with draw ratio for both the treated and untreated fibers. High f_a values are not obtained in the CO_2 treated fibers until the highest draw ratios are achieved where the TDR $>$ 11. The development of the amorphous orientation is much slower for the CO_2 treated fibers. This is a direct consequence of the low orientation produced during the first stage draw. Although the amorphous orientation develops relatively slow, the CO_2 treated fibers have slightly higher f_a values compared to the CO_2 treated fibers at DR_{max} values. Overall, the amorphous orientation for both fibers is quite high.

The amorphous orientation is probably not an optimum

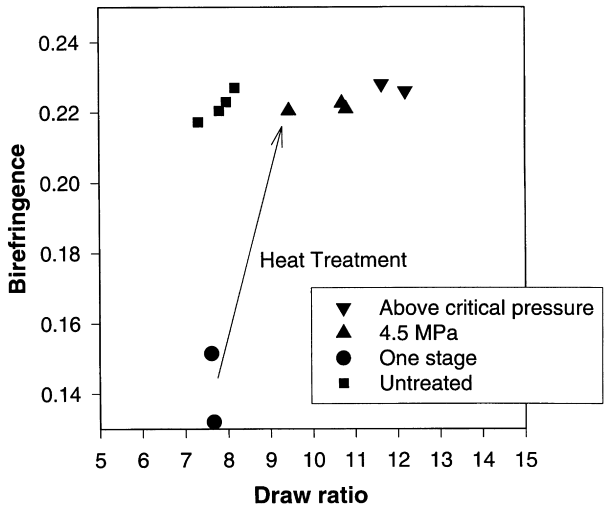

Fig. 5. Birefringence vs. draw ratio for CO_2-drawn and untreated fibers.

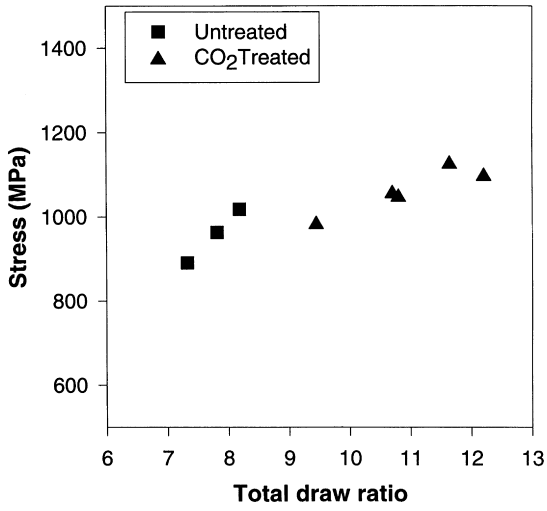

Fig. 7. Dependence of ultimate tensile strength on total draw ratio.

due to the use of a constant strain drawing technique. Ito et al. has shown that load upon drawing is a critical factor which affects the orientation in the noncrystalline regions and the final tensile properties as well [21]. Constant strain drawing can reach fairly high stress levels in the fibers as the maximum achievable draw ratio is approached. However, the load after constant strain drawing can decrease upon cooling allowing for relaxation and sub-optimum conditions.

3.4. Mechanical properties

The CO_2 treated fibers (~95 atm) show superior mechanical properties compared to untreated fibers. The treated fibers show superior tensile strength and moduli. Fig. 7 shows the development of tensile strength of PET fibers as a function of draw ratio after two-stage drawing. At the maximum achievable draw ratio, the fibers have a tensile strength of 1.1 GPa compared to 1.0 for untreated fibers, ~10% increase. These strength values are the upper limit for commercial PET resins primarily due to the relatively low molecular weight of polymer.

The tensile properties of PET are known to be dependent on the TDR, sample geometry, and the load applied on cooling [21]. Samples drawn to higher draw ratios such as CO_2 fibers can usually be drawn under higher true stress values. Higher drawing stresses or loads can be achieved with smaller cross sectional areas. For drawing conditions at constant strain rates, the tensile load usually reaches a plateau before the maximum draw ratio is achieved.

The moduli of the treated and untreated fibers are shown in Fig. 8. The tensile moduli of the treated fibers do not change significantly with draw ratio. This is due to similar stress levels achieved at the end of the drawing stage. It should be noted that the single filaments display a yield region in the stress vs. strain curves obtained. The modulus

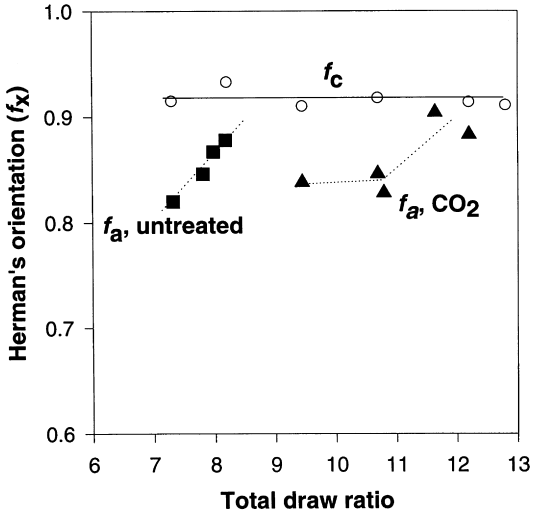

Fig. 6. Development of crystalline and amorphous orientation.

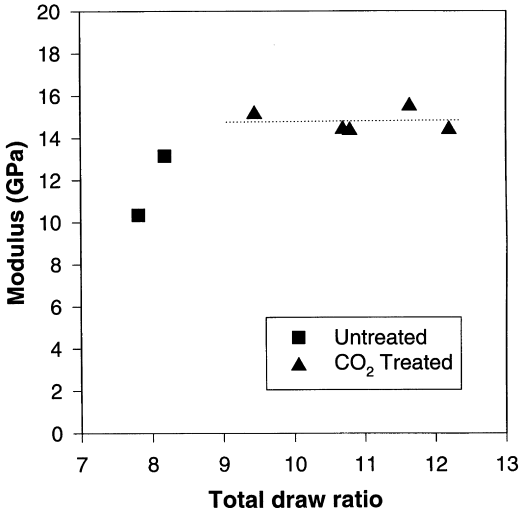

Fig. 8. Measure modulus values for treated and untreated fibers.

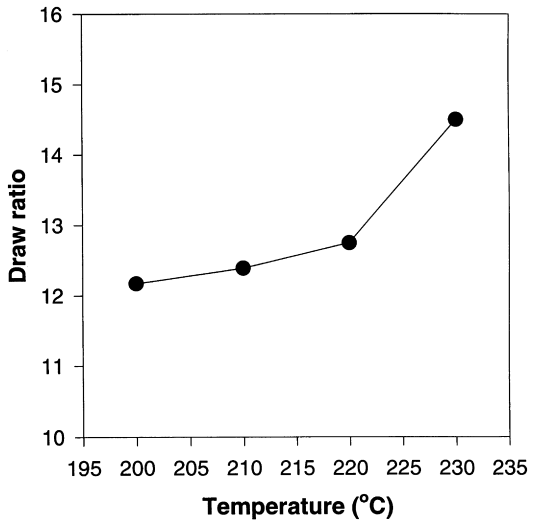

Fig. 9. Dependence of maximum achievable draw ratio on temperature.

values in Fig. 8 are within or above the range of modulus values reported for commercial PET fibers [22].

3.5. Temperature effects

Temperature dramatically affects crystallinity as discussed previously. The maximum achievable draw ratio is also temperature dependent. We were able to achieve a draw ratio of 14.4 at 230°C. Overall, the maximum achievable draw ratio increases with draw temperature as shown in Fig. 9. Untreated fibers can be drawn to only slightly higher draw ratios (~9) as reported previously at this temperature [23]. We confirmed this experimentally as well. We believe that improved drawability is associated with the entanglements and structure in the amorphous phase.

Temperature does have a large effect on the structure and mechanical behavior of PET fibers prepared using CO_2. Tensile strength of the fibers decrease as the second stage drawing temperature increases above 200°C. However, the tensile modulus increases along with the crystallinity. These results are highlighted in Table 2. While the crystalline orientation does not change, the amorphous orientation decreases significantly from 0.90 at 200°C to 0.66 at 220°C. Overall, temperature is one of the most important parameters that affects fiber structure and properties.

Initially, the tensile properties and birefringence of fibers drawn at higher temperatures were low due to hydrolysis. If the fibers were dried at 45°C for 36 h, the DR_{max} at higher temperatures was slightly lower and the tensile properties were significantly higher. At higher temperatures, hydrolysis may be one of several factors causing chain scission. However, loss of molecular weight with heat treatment has also been documented with melt and solution spun fibers which were dried prior to heat treatment [5]. Chain slippage may accompany molecular weight loss as well resulting in poor draw efficiency.

Another important factor on the final tensile properties of a given fiber is the load during cooling. The effects on tensile strength and modulus have been documented for various PET fibers [24]. For constant strain rate drawing, the maximum load achieved is dependent on temperature. We observed that as drawing temperature increases, the maximum load for a given cross sectional area achieved upon drawing decreases. This is undesirable because lower loads upon cooling result in lower amorphous orientation and strength values. For constant strain rate drawing, temperature can be controlled to balance crystallinity and amorphous orientation in order to optimize tensile properties.

3.6. Comparison to solvent treated fibers

Two primary differences exist between the second stage draw techniques used for CO_2 and solvent treated (acetone, DMF/H_2O) fibers. They are strain rate condition and heat treatment (duration and temperature). CO_2 treated fibers were drawn under constant strain rate conditions at 200°C. We also performed experiments at 230°C for a more direct comparison to solvent treated fibers. Acetone treated fibers were drawn under constant load conditions at 230°C. A constant load condition based on viscoelasticity results in nonlinear strain rates. The heat treatment time for the solvent treatment fibers is not known. The structural and tensile properties for CO_2 and solvent treated fibers are shown in Table 2. The values for solvent treated fibers are based on work by Ito et al. [25,26].

All of the modulus values measured in our laboratory (bold typeset in Table 2) are significantly lower than Ito's values. This may be due to the drawing method where constant load drawing creates a very high initial modulus at 0.1% strain. For CO_2 treated fibers, the measured modulus

Table 2
Comparison of PET fibers

Sample	Temperature (°C)	TDR	X_c (%)	f_c	f_a	Modulus (GPa)	Strength (GPa)
Untreated	200	8.2	53	0.933	0.881	13	1.0
CO_2	200	12.2	56	0.914	0.904	15	1.1
Untreated	230	8.5	50	0.887	0.980	24	1.0
CO_2	220	12.5	62	0.911	0.662	17	1.0
CO_2	230	14	65	0.925	0.621	16	0.9
Acetone	230	10.0	68	0.896	0.585	27	1.2
DMF/H_2O	230	11.5	–	–	–	28	1.2

values are closer to the values reported for commercially available fibers [27]. The modulus for the untreated fiber at 200°C is the same as commercial PET tire-grade fibers.

CO_2 treated fibers have better drawability and similar structural characteristics compared to solvent treated fibers. The degree of crystallinity for the CO_2 fibers is slightly lower at 230°C compared to a acetone treated fibers. Both fibers, however, show much larger crystallinity values ($\geq 65\%$) compared to untreated and commercial PET fibers($\sim 52\%$). The tensile strength values of the CO_2 treated fiber are lower compared to solvent treated fibers. We believe that this may be related to molecular weight and the time of temperature exposure during the second stage. At higher temperatures above 200°C, degradation is know to occur which can lower tensile properties [28].

The structural characteristics, f_a and f_c are very similar for the CO_2 and solvent treated fibers. For both of these, the f_a values are significantly lower than untreated fibers probably due to the initial morphology and low amorphous orientation after the first stage draw. Overall, drawing in CO_2 seems to be very similar compared to drawing in the presence of acetone or DMF/water mixture. While the processing conditions were not optimized, fibers with superior mechanical properties were obtained in comparison to untreated and most commercial fibers.

4. Conclusions

A two-stage draw technique was used for drawing both originally amorphous fibers and fibers which were drawn in situ in CO_2. The morphology of PET fibers drawn in CO_2 dramatically affects the final properties of the fiber after a second stage draw. CO_2 drawn fibers could be drawn to 50% higher draw ratios attaining higher strength, crystallinity, and orientation. The CO_2-induced morphology enhanced the development of the crystalline phase. At a draw temperature of 230°C, fibers with very high crystallinity values (65%) could be obtained. These fibers had very similar structural characteristics compared to acetone or DMF/water treated fibers. Both had a high crystalline orientation ($f_c > 0.9$) and a significantly lower amorphous orientation compared to untreated fibers. Overall, CO_2 drawn fibers have a distinct morphology dependent on the first stage drawing process. CO_2 can be used effectively for the processing and production of high performance PET fibers.

Acknowledgements

The authors acknowledge the National Science Foundation Materials Research Science and Engineering Center at the University of Massachusetts and financial support from the University of Massachusetts. We also thank Professor Richard Farris for the use of his laboratory facilities.

References

[1] Pereira JRC, Porter RS. J Polym Sci, Polym Phys Ed 1983;21:1133.
[2] Kunugi T, Suzuki A, Hashimoto M. J Appl Polym Sci 1981;26:1951.
[3] Amano M, Nakagawa K. Polymer 1986;27:429.
[4] Kunugi T, Suzuki A. J Appl Polym Sci 1996;62:713.
[5] Ito M, Takahashi K, Kanamoto T. J Appl Polym Sci 1990;40:1257.
[6] Wu G, Cuculo J. J Appl Polym Sci 1995;56:869.
[7] Ito M, Hosoi H, Kanamoto T. Polymer 1992;33:2575.
[8] Ito M, Miya H, Wanatobe M, Kanamoto T. J Appl Polym Sci 1990;40:543.
[9] Hobbs T, Lesser AJ. J Polym Sci, Part B: Polym Phys 1999;37:1881–91.
[10] Zachariades AE, Porter RS. J Appl Polym Sci 1979;24:1371.
[11] Wang LH, Porter RS. J Polym Sci, Polym Phys Ed 1984;22:1645.
[12] Ito M, Tanaka K, Kanamoto T. J Polym Sci, Polym Phys Ed 1987;25:2127.
[13] De R, Duibeny P, Bun CW, Brown CJ. Proc R Soc London, Ser A 1955;226:531.
[14] Huang B, Tucker P, Cuculo J. Polymer 1997;38:1103.
[15] Sun T, Desper R, Porter RS. J Mater Sci 1986;21:803.
[16] Ito M, Miya H, Wanatobe M, Kanamoto T. J Appl Polym Sci 1990;40:543.
[17] Mesiteri G, Del Nobile MA, Guerra G, Apicella A, Al Ghatta H. Polym Engng Sci 1995;35:506–7.
[18] Ito M, Hosoi H, Kanamoto T. Polymer 1992;33:2575.
[19] Ito M, Miya H, Wanatobe M, Kanamoto T. J Appl Polym Sci 1990;40:551–2.
[20] Ito M, Hosoi H, Kanamoto T. Polymer 1992;33:2576.
[21] Ito M, Takahashi K, Kanamoto T. Polymer 1990;31:61.
[22] Wu G, Tucker P, Cuculo J. Polymer 1997;38:1099.
[23] Ito M, Hosoi H, Kanamoto T. Polymer 1992;33:2575.
[24] Ito M, Takahashi K, Kanamoto T. Polymer 1990;31:60.
[25] Ito M, Hosoi H, Kanamoto T. Polymer 1992;33:2575.
[26] Ito M, Miya H, Wanatobe M, Kanamoto T. J Appl Polym Sci 1990;40:543.
[27] Wu G, Tucker P, Cuculo J. Polymer 1997;38:1099.
[28] Ito M, Miya H, Wanatobe M, Kanamoto T. J Appl Polym Sci 1990;40:552.